Bulletin of Mathematical Biology Vol. 53, No. 6, pp. 881–899, 1991.
Printed in Great Britain.

0092-8240/91$3.00+0.00
Pergamon Press plc

ONE-WAY BLOCKS IN CARDIAC TISSUE: A MECHANISM FOR PROPAGATION FAILURE IN PURKINJE FIBRES

■ M. A. LEWIS* and P. GRINDROD†
Centre for Mathematical Biology,
Mathematical Institute,
24–29 St. Giles',
Oxford, OX1 3LB, U.K.

(*E.mail: lewis@amath.washington.edu*)

The concept of a one-way block, arising from a region of depressed tissue, has remained central to theories for cardiac arrhythmias. We show that both the geometry of a depressed region and spatial heterogeneities in depression are key factors for inducing such a block. By using an asymptotic approximation, known as the eikonal equation, to model qualitatively the movement of a depolarization wave-front down a Purkinje fibre bundle, we show how a one-way block in conduction may result from asymmetric constriction in the width of a depressed bundle. We demonstrate that this theory is valid for biologically relevant parameters and simulate a one-way block by numerically solving the eikonal approximation. We consider the case of non-uniform depression, where the planar travelling wave speed is spatially dependent. Here, numerical simulations indicate that such a spatial dependency may, in itself, be sufficient to produce a one-way block.

1. Introduction. The cause of ventricular fibrillation has been of widespread experimental and theoretical interest. One of the longest standing theories for fibrillation is that it arises from the generation of one-way re-entrant excitable waves, known as circus excitation waves. These waves are not usually present in a healthy heart, but it is possible that the right physiological conditions coupled with an appropriate stimulus would give rise to them. Once they were initiated they would interrupt the normal rhythmic behaviour of the heart and would eventually lead to fibrillation, or rapid chaotic contractions, and ultimately death.

Ashman and Hull (1945) suggested how circus excitation might arise from a myocardial infarct, or island of tissue which is damaged by anoxia or disease. The tissue in this island would be less excitable than the surrounding myocardium and would therefore conduct impulses more slowly. The island would also have to sustain a one-way block; waves would only be able to enter

* Present address: Department of Applied Maths FS-20 and Department of Zoology NJ-15, University of Washington, Seattle, WA 98195, U.S.A.

† Present address: Intera-Sciences, Environmental Sciences Department, Chiltern House, 45 Station Road, Henley-on-Thames, Oxfordshire, RG9 1AT, U.K.

the island from one side. A wave of excitation would reach the infarct and sweep around it, to find an entrance only on one side. The impulse would then creep through the island slowly before reaching the border and exiting through the one-way block. The tissue would have had time to recover excitability and the excitation wave would continue to circulate. Ashman and Hull recognized clearly that re-entry cannot occur unless there is a partly isolated pathway in which conduction is unidirectional.

Although one-way blocks have been experimentally observed in cardiac tissue for many years (Schmitt and Erlanger, 1928), it was not until the work of Wit and co-workers (1972a,b) that circus movements of excitation, arising from slow conduction and a one-way block, were experimentally shown to occur under conditions which might arise *in situ* in the heart; sustained movements of excitation were observed around relatively short loops of Purkinje fibre bundles exposed to high potassium and epinephrine.

The concept of a one-way block has remained central in recent theories for cardiac arrythmias, although it is sometimes considered to be a dynamic phenomenon which is due to time-dependent spatial gradients (Allessie *et al.*, 1977; Winfree, 1983; Chen *et al.*, 1988). The question of how these blocks can arise is crucial to understanding the theory of circus excitations and their relation to cardiac arrythmias.

Cranefield (1975) indicates that asymmetry of conduction is a normally occurring phenomenon in cardiac tissue; accurate measurements show that even wholly normal fibre bundles exhibit some asymmetry of conduction. However, depression of excitability magnifies this asymmetry until a one-way block may eventually occur. This is supported by experimental results (Cranefield *et al.*, 1971), which show that the immersion of a Purkinje fibre bundle in a high potassium chloride Tyrode's solution can lead to depressed excitability and thus to the slow conduction of characteristic depolarization impulses. Conduction is not only slow but asymmetrical, conduction in one direction being slower than in the other direction. Severe depression leads to a one-way block, or the inability of the fibre bundle to transmit impulses in one direction.

The movement of excitable waves through fibres of variable radius, excitability or resistivity have been investigated numerically (Joyner, 1981; Miller, 1979) and via phase plane arguments (Keener, 1984). Results indicate that abrupt asymmetrical changes in such properties may result in one-way transmission blocks.

A recent asymptotic result, known as the *eikonal* equation for reaction diffusion systems (Keener, 1986), shows that the normal velocity of a wave of excitation depends on the shape of the wave-front boundary layer (wave boundary). The eikonal equation relates the normal velocity (N) to the planar travelling wave speed (c) and the curvature (κ) of the wave boundary. The

normal velocity is decreased in regions of positive curvature, and is increased in regions of negative curvature. Keener (1987) suggested that this velocity–curvature relationship could be used in finding conditions for one-way transmission blocks in excitable fibres.

In a region of slow conduction, the shape of a wave boundary depends critically on the geometry of the region. Furthermore, curvature effects may act differently for waves moving in different directions. These curvature effects would be small (relative to the planar wave speed) for slightly depressed regions, but would become significant in highly depressed regions with a slow planar wave speed. This leads us to suggest that the geometry of the depressed area is the key factor which makes conduction asymmetric. By way of an example, we quantitatively model the effects of Purkinje fibre bundle geometry on conduction speeds, with particular reference to the effect of small asymmetric changes in fibre bundle diameter (Section 2). We also consider the effect that a spatially non-uniform depression of cardiac tissue may have on the formation of blocks (Section 3). In this case, the geometry of the non-uniform depression causes the block.

2. One-way Blocks in Purkinje Fibre Bundles

2.1. The physiology of Purkinje fibre bundles. Purkinje fibre bundles make up part of the electrical communication system in the heart. They are often studied in cardiology experiments as they are easy to excise and isolate and can be conveniently prepared for use in a tissue bath (Cranefield, 1975). Each fibre bundle is made up of individual fibres, or cells approximately 100 μ long and 10 μ wide (Sommer and Johnson, 1968).

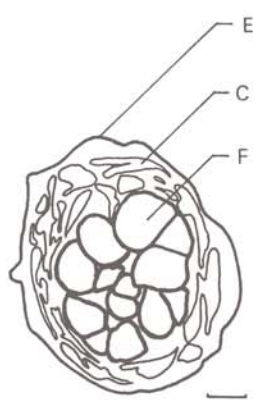

Figure 1. Transverse section through a rabbit Purkinje fibre bundle. The strand is surrounded by endocardium (E). Collagen (C) intermingled with fibrocytes and Schwann cells make up the next layer. The interior is composed of the fibres themselves (F). The horizontal bar represents 10 μ. The drawing is based on a photomicrograph from Johnson and Sommer (1967).

A cross-section of the bundle will reveal that it is comprised of 10 or so fibres, joined radially by nexus junctions (sometimes referred to as gap junctions; Mobley and Page, 1972; Johnson and Sommer, 1967), and is surrounded by a layer of endothelium (endocardium) (Fig. 1). Nexus junctions are regions where the plasma membranes of adjacent cells come into close apposition, leaving a 20 Å gap which can be delineated with lanthanum (Mobley and Page, 1972). The fact that the bundle is comprised of fibre sub-units means that the total membrane area is about 10 times that of the area of the surrounding endocardium (McAllister *et al.*, 1975).

These nexus junctions are generally assumed to be low resistance pathways for current flow between cells and not pathways for the flow of current between the inside and outside of cells (Mobley and Page, 1972). This is supported by the careful mapping of nexus junctions in a length of rabbit Purkinje fibre bundle (Sommer and Johnson, 1968). This mapping also indicates that the bundle may vary longitudinally, both in the number of individual fibres or cells and in the number of junctions between fibres. The fibre bundle radius depends on the number of fibre sub-units, the individual fibre radii and the proximity of adjacent fibres. In turn, the proximity of adjacent fibres in inter-junctional regions depends on the type of fibre bundle; adjacent fibres are more tightly packed in larger mammals, such as the sheep, goat and dog, and are less tightly packed in smaller mammals, such as the rabbit, guinea-pig and cat (Sommer and Johnson, 1968). However, the most commonly used value for the fibre bundle radius is 40 μ, which is suitable for sheep fibre bundles (Weidmann, 1952). Individual fibres are also joined longitudinally by nexus or similar junctions.

2.2. Model for electrical activity in Purkinje fibres. The electrical activity in Purkinje fibres is believed to arise from Hodgkin–Huxley-type voltage-dependent gate mechanisms which regulate ionic flows across the encasing membrane (McAllister *et al.*, 1975; Noble, 1962). These gate mechanisms regulate the ionic flows by voltage-dependent changes in membrane structure (Jack *et al.*, 1975). The resulting selective, voltage-dependent flows of sodium, potassium, calcium and chloride ions lead to an ionic current, I_{ion}, across the membrane. The voltage established across the membrane is proportional to the amount of charge separation, so that a capacitive current flow, I_{cap}, determines the rate at which the voltage changes, that is, $\partial V/\partial t$.

The total current flow across the membrane, I_{mem}, is the sum of the ionic and capacitive currents. Thus:

$$I_{\text{mem}} = I_{\text{cap}} + I_{\text{ion}} = C_{\text{m}} \frac{\partial V}{\partial t} + I_{\text{ion}},$$

where C_{m} is the membrane capacitance and V is the voltage (Jack *et al.*, 1975).

Application of Ohm's Law and Kirchhoff's Law gives the N-dimensional cable equation:

$$\sum_{j=1}^{N} \frac{1}{R_j} \frac{\partial^2 V}{\partial x_j^2} = \rho I_{\text{mem}} = \rho C_{\text{m}} \frac{\partial V}{\partial t} + \rho I_{\text{ion}}, \tag{1}$$

where x_j is the jth space component, R_j is the intracellular resistivity in the x_jth direction and ρ is a proportionality constant which gives the relation between membrane area A and volume V as $\mathrm{d}A = \rho\, \mathrm{d}V$. The choice of $N=1$, $\rho = 2/a$ and $I_{\text{ion}} = V/R_{\text{m}}$ where R_{m} is the membrane resistance and a is fibre radius gives the classical one-dimensional linear cable equation.

In the case of Purkinje fibres, however, experimental evidence shows that the relationship between I_{ion} and V is both time-dependent and highly non-linear (McAllister *et al.*, 1975). These dynamics lead to an excitable action potential; when the fibre is electrically stimulated a rapid depolarization, or upstroke, is followed by a slow repolarization back to a negative potential. In a healthy Purkinje fibre, the rapid depolarization takes less than 1 ms, while the repolarization stage takes the order of a second (McAllister *et al.*, 1975). Hunter *et al.* (1975) suggested that, although the current–voltage relationship in a Purkinje fibre is time-dependent, the essential characteristics of the rapid depolarization upstroke could still be retained by dropping the time dependency and choosing $I_{\text{ion}} = f(V)$, where:

$$f(V) = g(V - V_{\text{r}}) \left(1 - \left(\frac{V - V_{\text{r}}}{V_{\text{th}} - V_{\text{r}}}\right)^2\right) \left(1 - \left(\frac{V - V_{\text{r}}}{V_{\text{p}} - V_{\text{r}}}\right)^2\right), \tag{2}$$

where V_{r} is the resting potential (-90 mV), V_{th} is the threshold potential (-67 mV), V_{p} is the peak voltage attained during depolarization (47 mV) and g is a scaling factor. This $f(V)$ was substituted into the one-dimensional cable equation [see equation (1)] and the speed of the rapid depolarization upstroke was analytically estimated. Switching to a travelling wave coordinate system gave an ordinary differential equation and the appropriate application of boundary conditions determined the speed uniquely.

A single Purkinje fibre is typically considered to be a one-dimensional system. Although the fibres are *individually* considered to be one-dimensional, it is necessary to use a three-dimensional model when considering how geometry affects the conduction velocity of a depolarization front moving through a *bundle* of interconnected fibres. In this case we choose the ionic current–voltage relationship in the depolarization front to be the appropriate "N-shaped" curve, given by $I_{\text{ion}} = f(V)$, where $f(V)$ has zeroes at V_{r}, V_{th} and V_{p}, but is not explicitly given. Therefore our model retains a degree of robustness by not stating $f(V)$ exactly. However, it is important that $f(V)$ is "N-shaped" so as to give excitable dynamics. Thus,

$$\frac{1}{R_x}\frac{\partial^2 V}{\partial x^2}+\frac{1}{R_y}\frac{\partial^2 V}{\partial y^2}+\frac{1}{R_z}\frac{\partial^2 V}{\partial z^2}=\rho C_m\frac{\partial V}{\partial t}+\rho f(V) \tag{3}$$

models the movement of the depolarization front through the three-dimensional structure of the Purkinje bundle. Longitudinal depolarization is effected by the action potential moving along the individual fibres and through longitudinal nexus junctions (in the x-direction) and lateral depolarization (in the y- and z-directions) is effected through the interconnecting lateral nexus junctions. The fact that the exterior fibres of the Purkinje bundle are not electrotonically connected to the extracellular fluid by nexus junctions suggests zero-flux boundary conditions for V along the exterior of the bundle.

2.3. Curvature correction for bundle widening. Results from Sommer and Johnson (1968) indicate that Purkinje fibre bundles are not longitudinally uniform. The number of fibre sub-units varied between nine and 13 over an observed length of 160 μ. These variations are incorporated into the three-dimensional model by an effective change in fibre bundle width. If we assume that the bundle is radially symmetric, then the bundle radius can be given as $a(x)$, where x is the longitudinal axis and $0\leqslant\sqrt{y^2+z^2}\leqslant a(x)$.

To understand the effect of a bundle widening on the speed of the depolarization wave in the x-direction, N_x, we choose the simplest possible geometry. This is given by a uniform bundle with radius a_0 which widens by an angle α (Fig. 2). We assume radial isotropy ($R_y=R_z=R$), but longitudinal anisotropy ($R_x\neq R$).

We non-dimensionalize the model (3) to a form which is suitable for the analysis of such a geometry by choosing:

$$x^*=\frac{x}{a_0}\sqrt{\frac{R_x}{R}},\quad y^*=\frac{y}{a_0},\quad z^*=\frac{z}{a_0},\quad t^*=\frac{t}{a_0 C_m R},$$

$$V^*=\frac{V-V_r}{V_p-V_r},\quad f^*=\frac{-R}{\rho(V_p-V_r)}f,\quad \varepsilon=\frac{1}{a_0\rho}.$$

This puts the anisotropic tissue in exact correspondence with isotropic media, while f^* is a familiar non-linear excitation curve with zeroes at $V^*=0$, $V^*=(V_{th}-V_r)/(V_p-V_r)$ and $V^*=1$ (Fig. 3). In this non-dimensional system, the fibre bundle widens by the angle α^*, given by:

$$\sin(\alpha^*)=\frac{\sqrt{\dfrac{R}{R_x}}\tan(\alpha)}{\left(1+\left(\dfrac{R}{R_x}\right)\tan^2(\alpha)\right)^{1/2}}. \tag{4}$$

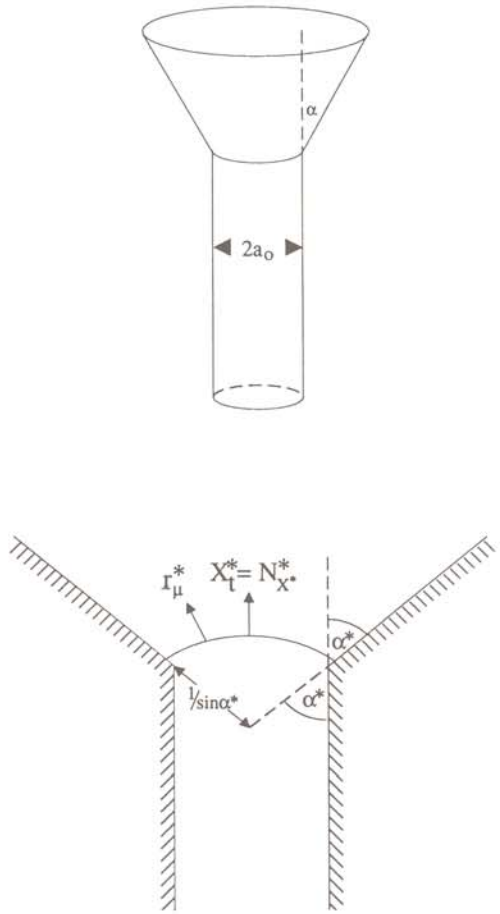

Figure 2. Geometry of bundle widening. (a) A uniform bundle, with radius a_0, widens by an angle α. (b) The analogous widening in non-dimensional coordinates, shown in the $z^*=0$ longitudinal section. Movement of the wave boundary [given by $\mathbf{r}^*(0, \eta, \lambda, t)=0$] is described in (7). $N^*_{x^*}$ is the speed of the wave in the x^*-direction, measured at the point $y^*_\mu=z^*_\mu=0$.

The fact that the total membrane area is about 10 times that of the external surface of the bundle (Section 2.1) means that the non-dimensional scaling variable $\varepsilon \approx 0.05$. Thus equation (3) can be rewritten as:

$$\varepsilon \frac{\partial V^*}{\partial t^*} = \varepsilon^2 \left(\frac{\partial^2 V^*}{\partial x^{*2}} + \frac{\partial^2 V^*}{\partial y^{*2}} + \frac{\partial^2 V^*}{\partial z^{*2}} \right) + f^*(V^*), \tag{5}$$

with zero-flux boundary conditions for V^* along the exterior of the bundle.

2.4. Eikonal formulation. We introduce the moving coordinate system:

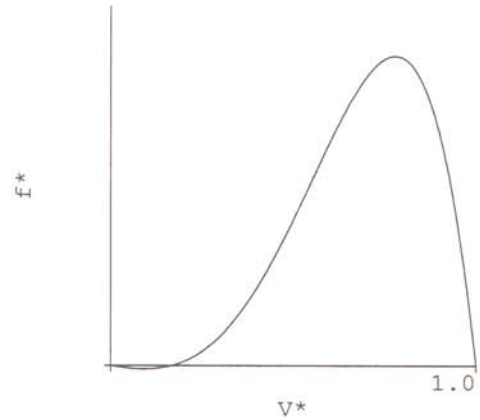

Figure 3. Non-linear excitation curve for a Purkinje fibre bundle. The non-dimensional current–voltage relationship for the rapid depolarization upstroke in a Purkinje fibre bundle is shown [see (2) and (5)]. Based on Hunter *et al.* (1975).

$$\mathbf{r}^* = \begin{pmatrix} x^*(\mu, \eta, \lambda, t) \\ y^*(\mu, \eta, \lambda, t) \\ z^*(\mu, \eta, \lambda, t) \end{pmatrix}$$

where $\{\mu, \eta, \lambda\}$ constitutes a triply orthogonal system of coordinates:

$$\mathbf{r}^*_\mu \cdot \mathbf{r}^*_\lambda = 0, \quad \mathbf{r}^*_\lambda \cdot \mathbf{r}^*_\eta = 0, \quad \mathbf{r}^*_\eta \cdot \mathbf{r}^*_\mu = 0, \quad |\mathbf{r}^*_\mu| = 1,$$

$\mathbf{r}^*_\mu = \partial \mathbf{r}^*/\partial \mu$, and similarly for $\mathbf{r}^*_\lambda$ and $\mathbf{r}^*_\eta$. At any time, t, the surface given by $\mathbf{r}^*(0, \eta, \lambda, t)$ is the wave boundary parameterized by η and λ. Thus:

$$\mathbf{r}^*_\mu = \frac{\mathbf{r}^*_\eta \times \mathbf{r}^*_\lambda}{|\mathbf{r}^*_\eta| \, |\mathbf{r}^*_\lambda|} \tag{6}$$

is the unit vector normal to the wave boundary, and:

$$\mathbf{r}^*_t = N^* \mathbf{r}^*_\mu, \tag{7}$$

where N^* is the normal velocity of the wave boundary in the non-dimensionalized system.

Following the procedure in Gomatam and Grindrod (1987), we use the stretched coordinate $\xi = \mu/\varepsilon$ to find solutions of the form $V = V(\xi)$, and arrive at an asymptotic approximation for N^* in terms of the one-dimensional travelling wave speed, denoted by c^*, and twice the mean curvature of the wave boundary, denoted by κ^*, in the non-dimensionalized system. This approximation is given by:

$$N^* = c^* - \varepsilon \kappa^*, \tag{8}$$

where:

$$\kappa^* = -\frac{\mathbf{r}^*_{\eta\eta}\cdot(\mathbf{r}^*_\eta \times \mathbf{r}^*_\lambda)}{|\mathbf{r}^*_\eta|^3|\mathbf{r}^*_\lambda|} - \frac{\mathbf{r}^*_{\lambda\lambda}\cdot(\mathbf{r}^*_\eta \times \mathbf{r}^*_\lambda)}{|\mathbf{r}^*_\eta||\mathbf{r}^*_\lambda|^3} \tag{9}$$

is referred to as the *eikonal* equation for reaction diffusion systems and is valid to $\mathcal{O}(\varepsilon^2)$. Thus equations (6), (7), (8) and (9) predict the time evolution of the wave boundary.

The specific form of the time evolution equation depends on the solution domain. For example, if we solve over the infinite plane, then:

$$x^*_t = \left(c^* + \varepsilon \frac{x^*_{\eta\eta}y^*_\eta - y^*_{\eta\eta}x^*_\eta}{(x^{*2}_\eta + y^{*2}_\eta)^{3/2}}\right)\frac{y^*_\eta}{(x^{*2}_\eta + y^{*2}_\eta)^{1/2}} \tag{10}$$

$$y^*_t = \left(c^* + \varepsilon \frac{x^*_{\eta\eta}y^*_\eta - y^*_{\eta\eta}x^*_\eta}{(x^{*2}_\eta + y^{*2}_\eta)^{3/2}}\right)\frac{-x^*_\eta}{(x^{*2}_\eta + y^{*2}_\eta)^{1/2}} \tag{11}$$

(Keener, 1986). This system can be conveniently solved by finite difference methods (Grindrod *et al.*, 1991). We use this two-dimensional form of the time evolution equation for subsequent numerical simulations, rather than the full three-dimensional system given by equations (6), (7), (8) and (9). Numerical solution of the cylindrically symmetrical three-dimensional equations may also be possible and will be the subject of further work.

The speed of the depolarization wave in the x^*-direction, $N^*_{x^*}$, is given by the value of N^* at $y^*_\mu = z^*_\mu = 0$. We let $\kappa^*_{x^*}$ denote the curvature correction term at this point. In the dimensional system, the corresponding speed, N_x, and curvature correction term, κ_x, have units cm/ms. When we evaluate (7) at $y^*_\mu = z^*_\mu = 0$, we have:

$$x_t = N_x$$

where:

$$N_x = c_x - \varepsilon\kappa_x,$$

c_x is the planar travelling wave speed in the x-direction and:

$$\kappa_x = \frac{\kappa^*_{x^*}}{C_m\sqrt{RR_x}}. \tag{12}$$

This is the time evolution equation for a point on the wave boundary whose normal vector points in the x-direction, and thereby models the speed of the depolarization wave in the x-direction.

The symmetry of the asymptotic solution for V along the wave boundary means that the zero-flux boundary conditions in (5) constrain the wave

boundary to intersect perpendicularly with the bundle wall. If we introduce a scalar field, $g(x^*, y^*, z^*)$, which defines the bundle wall by $g=0$, then, provided ∇g is non-vanishing along the bundle wall, we can write this constraint as:

$$\nabla g \cdot \mathbf{r}_{\mu}^{*}=0$$

at $g=0$. It is evident that if such an intersection were non-orthogonal, then the zero-flux boundary conditions would be violated at the point of intersection (Grindrod *et al.*, 1991). The effect of this orthogonality constraint is to cause an increase in mean curvature and a subsequent slowing of the wave boundary as it passes through the widening (Fig. 2). However, the value of $\kappa_{x^*}^{*}$ is bounded above by $2\sin(\alpha^*)$, which is realized only when α^* is just large enough to stop the wave front completely through curvature effects. Thus from equations (4) and (12) we see that:

$$(\kappa_x)^2 \leqslant (\kappa_m)^2 = \frac{\tan^2(\alpha)}{q_0^2(1+r_0\tan^2(\alpha))}, \tag{13}$$

where $q_0=(C_m R_x)/2$ and $r_0=R/R_x$.

Approximate values for C_m and R_x in Purkinje fibre bundles are 1 μF/cm^2 and 0.1 kΩ cm respectively (Weidmann, 1952; McAllister *et al.*, 1975). Using these values, q_0 is calculated to be approximately 0.05 ms/cm.

The value for R is much harder to determine. However, Freygang and Trautwein (1970) give results which allow a very rough estimate. Based on phase-angle response data, the effective radial resistance in a Purkinje fibre bundle is roughly calculated to be $R=60$ kΩ cm, thus making r_0 approximately 600. This means that the longitudinal speed of the impulse is ≈ 25 times the radial speed [see equation (3)]. This indicates a considerably larger degree of anisotropy than in myocardial tissue, where the speed of the impulse is approximately three times faster in the longitudinal direction than in the transverse direction (Clerc, 1976). However, there is a fundamental structural difference between myocardial and Purkinje fibres; ventricular myocardial fibres have transverse tubule connections (T-tubules) which are absent in Purkinje fibres. These effectively join the myoplasm of adjacent fibres (Sommer and Johnson, 1968) and thereby electrotonically couple them in a manner which is not found in Purkinje fibres.

The relationship between κ_m and α, given in equation (13), is shown in Fig. 4. The relatively large degree of anisotropy ($r_0=600$) means that κ_m quickly asymptotes to approximately $\sqrt{2/3}$ cm/ms as α increases. Therefore we expect the curvature correction term, $\varepsilon\kappa_x$, to be in the range -0.04 cm/ms $\leqslant \varepsilon\kappa_x \leqslant$ 0.04 cm/ms.

It is important to note that the curvature effects arising from variations in bundle diameter only affect the wave speed over the short length where the

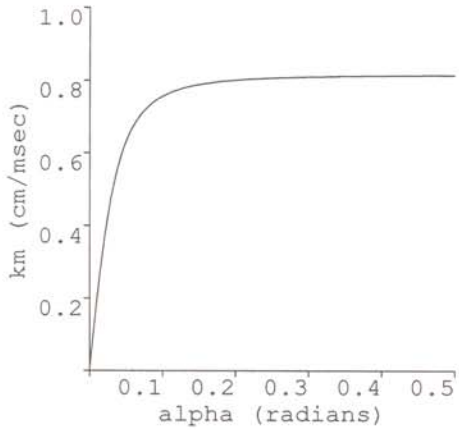

Figure 4. The maximum curvature correction, κ_m, given as a function of the widening angle, α, for $q_0 = 0.05$ ms/cm and $r_0 = 600$ (13). The relatively large degree of anisotropy means that κ_m quickly asymptotes to $\sqrt{2/3}$ cm/ms.

diameter is actually changing; the remaining portion of bundle length supports a wave with the planar travelling wave speed c_x. The effect of a widening is to slow the wave temporarily, while the effect of a narrowing is to increase the wave speed temporarily. The average wave speed between the points $a \leqslant x \leqslant b$, is given by:

$$N_x^{av} = \left(\frac{1}{b-a} \int_a^b \frac{dx}{N_x} \right)^{-1} = \left(\frac{C_m \sqrt{RR_x}}{b-a} \int_a^b \frac{dx}{c^* - \varepsilon \kappa_{x^*}^*} \right)^{-1}. \tag{14}$$

Typically, the effect of a symmetric narrowing and widening (constriction) will decrease the average wave speed. This is clearly illustrated in the extreme case where the widening is abrupt enough to stop the wave completely and the average speed drops to zero. Contributions by the integrand in (14) are directionally dependent because $\mathrm{sgn}(c^*)$ changes with direction while $\mathrm{sgn}(\kappa_x^*)$ does not. This means that asymmetric constrictions tend to reduce the average wave speed asymmetrically. In other words, the average wave speed depends on the direction in which it is measured. This is illustrated in Fig. 5, where the non-dimensionalized planar system (10) and (11) is solved numerically for waves moving through a constriction. Figure 6 shows how an asymmetric constriction in a bundle may be sufficient to produce a one-way block.

The average wave speed in healthy Purkinje fibre bundles is approximately 0.2 cm/ms (Weidmann, 1952; Cranefield, 1975). This average wave speed serves as a rough estimate for c_x in healthy fibres, although in general it will be an underestimate. Even in healthy fibre bundles, some asymmetry in average wave speed is observed (Cranefield *et al.*, 1971). We suggest that this reflects the asymmetries in the variations in bundle width, as discussed above. These

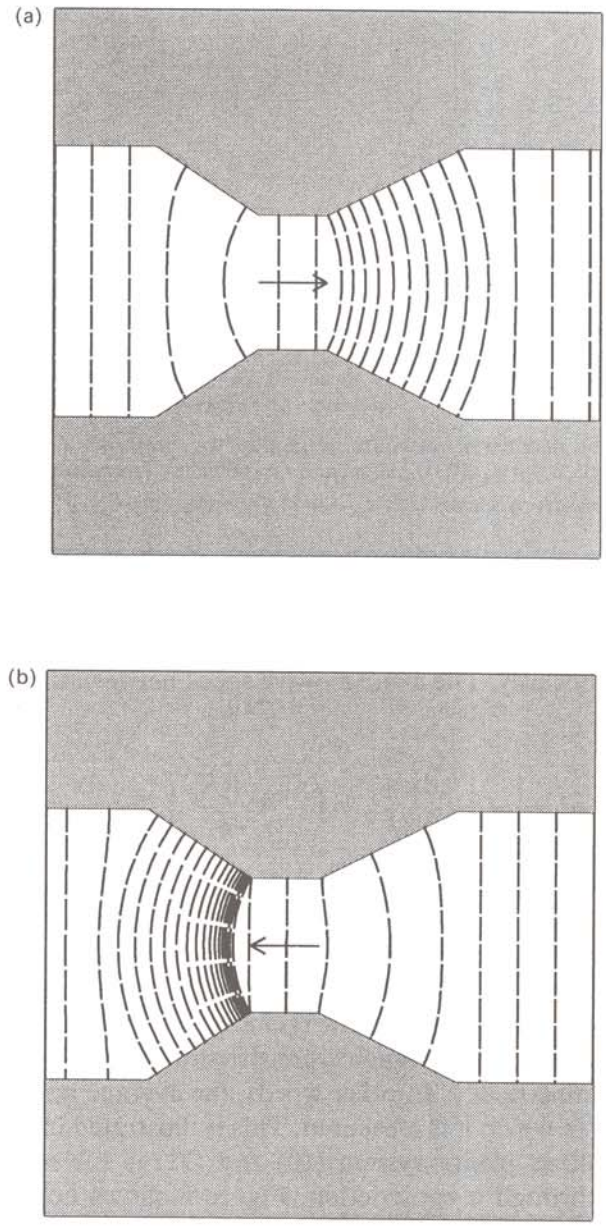

Figure 5. An asymmetric constriction in bundle width gives rise to directionally-dependent wave speeds. Numerical solution of (10) and (11) with orthogonal boundary conditions shows directionally-dependent slowing of the wave boundary as it passes through an asymmetric constriction. The average wave speed in the x^*-direction [see (a)] is approximately 1.37 times the average wave speed in the $-x^*$-direction [see (b)]. The fibre bundle constricts from a non-dimensional width of 1 to 0.5. The parameter values are $c^* = 0.055$ and $\varepsilon = 0.05$. Refer to the text and equation (14) for further explanation.

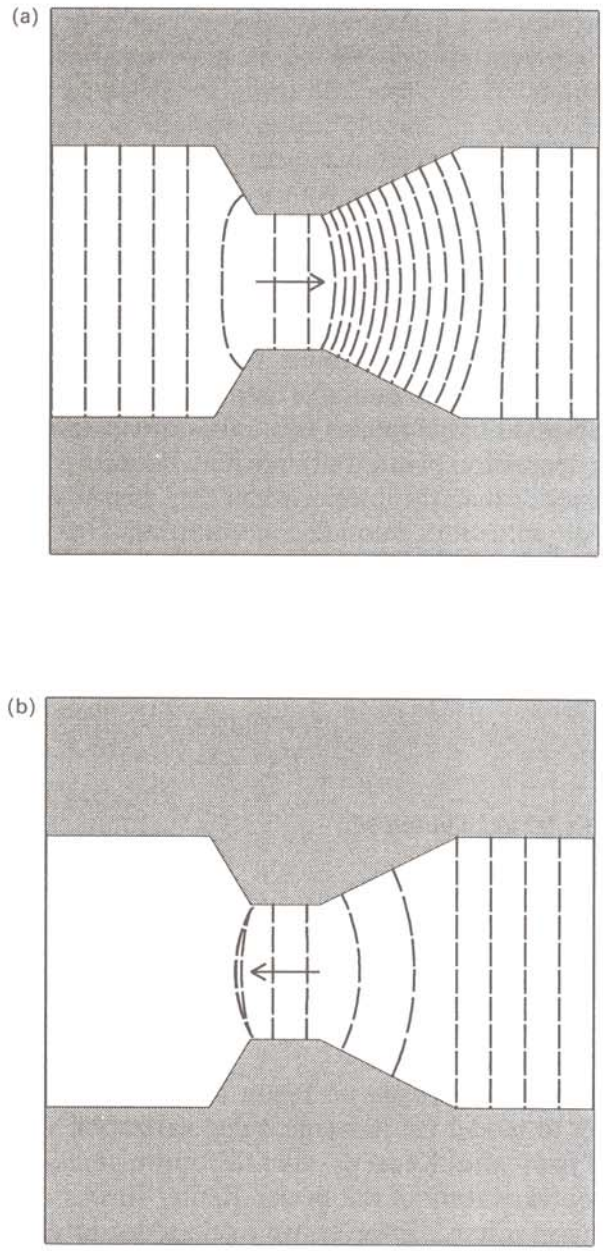

Figure 6. An asymmetric constriction in bundle width can be sufficient to produce a one-way block. Numerical solution of (10) and (11) with orthogonal boundary conditions shows how an asymmetric block may suffice in bringing the wave boundary to a complete standstill. Here, blockage is one-way; the wave passes freely through the constriction in the x^*-direction (a), but is blocked in the $-x^*$-direction (b). The fibre bundle constrict from a non-dimensional width of 1 to 0.5. The parameter values are $c^* = 0.05$ and $\varepsilon = 0.05$.

become more pronounced in depressed fibres (Cranefield, 1975); asymmetric wave speeds of 0.038 cm/ms vs 0.066 cm/ms have been observed in depressed dog Purkinje fibre bundles (Cranefield *et al.*, 1971), suggesting a pronounced directional asymmetry in bundle width variations. Other experimental evidence indicates that under certain conditions the average wave speed can be depressed to as low as 0.005 cm/ms before one-way blocks occur (Cranefield, 1975). In these cases, variations may be either small or may have only a slight directional asymmetry. These figures suggest that the range previously given for $\varepsilon\kappa_x$ ($-0.04 \leqslant \varepsilon\kappa_x \leqslant 0.04$) is of the right order of magnitude.

3. Non-uniform Depression of Excitable Tissue. So far, we have implicitly assumed that the depression of excitable tissue is spatially uniform. It is highly unlikely that depressed tissue retains this uniformity. Cranefield *et al.* (1971) suggest that the depression of dog Purkinje fibre bundles is more pronounced on the bundle exterior than the interior when they are subjected to a Tyrode's solution with high potassium chloride concentration. One would expect that any form of depression of cardiac tissue, whether through anoxia, disease or temporary refractoriness, would have some spatial variation. The planar travelling wave speed is thus, in turn, intrinsically a function of the depressed excitation dynamics. For example, the one-dimensional version of (5) yields:

$$c^* = \frac{\int_0^1 f^*(V^*)\,\mathrm{d}V^*}{\int_{-\infty}^{\infty} V_{\xi^*}^{*\,2}\,\mathrm{d}\xi^*},$$

where $\xi^* = (x^* + c^* t^*)/\varepsilon$. Therefore:

$$\operatorname{sgn}(c^*) = \operatorname{sgn}\left(\int_0^1 f^*(V^*)\,\mathrm{d}V^*\right). \tag{15}$$

In healthy tissue, (15) is positive (Fig. 2). However, severe depression may lead to a sign change. Thus, both the sign and magnitude of c^* depend on the excitation dynamics, given by f^*.

Here, we follow the approach of Tyson and Keener (1987) and use the eikonal equation to model the movement depolarization waves through the myocardium. Tyson and Keener's eikonal approximation arose from a reaction–diffusion caricature of the Beeler–Reuter (Beeler and Reuter, 1977) model for the myocardium. However, we retain a degree of flexibility by not linking the eikonal equation explicitly to its origins in a specific reaction–diffusion system; the only parameters that the original reaction–diffusion system yields are the planar travelling wave speed (c) and the scaling parameter for the dynamics (ε). Thus our eikonal equation model can be considered as an $\varepsilon\kappa$ refinement to modelling the myocardium with Huyghens principle ($N = c$; see Auger *et al.*, 1988). Based on our arguments for spatially non-uniform

depression, we assume that the movement of the wave boundary can be described qualitatively by a spatially dependent eikonal equation approximation:

$$N^* = c^*(x^*, y^*) - \varepsilon\kappa^*, \tag{16}$$

in a non-dimensional system which is chosen so as to put the anisotropic tissue in exact correspondence with the isotropic media. Here, the planar travelling wave speed, $c^*(x^*, y^*)$, depends on the spatial variation in the excitation dynamics, given by the instantaneous current–voltage relationship, $f^*(V^*)$. Note that the spatial dependence of $c^*(x^*, y^*)$ precludes a rigorous derivation of (16) from a reaction–diffusion system with spatially dependent excitation dynamics. However, we feel that this is justified as we are using (16) as a model rather than an asymptotic approximation.

By way of example, we numerically investigated an excitable system where there are two adjacent regions of depressed conduction. Based upon our analysis of directionally-dependent wave speeds in Purkinje fibres, we expect that, as the wave boundary exists from the channel between the depressed regions, its behaviour may be affected crucially by local spatial variations in the wave speed. Whereas abrupt changes in the spatially-dependent wave speed may retard or even stop the wave boundary, more gradual variations in the wave speed should facilitate a smooth exit. With this in mind, we anticipate that a one-way block may occur when $c^*(x^*, y^*)$ is chosen so that there is an abrupt exit in one direction, but a gradual exit in the other direction. Such directional asymmetry is exhibited by:

$$c^* = \begin{cases} \gamma^{1/4} & \text{if } y > 0, \\ \gamma & \text{otherwise,} \end{cases} \tag{17}$$

where:

$$\gamma = \frac{r_1 r_2}{r_1 + r_2 + r_1 r_2} + c_{\min},$$

$$r_1 = \sqrt{x^{*2} + y^{*2}},$$

$$r_2 = \sqrt{(x^* - 1)^2 + y^{*2}}$$

and $c_{\min} < 0$ on the domain $-1 \leqslant x^*, y^* \leqslant 1$ (Fig. 7).

Zero-flux boundary conditions were applied to the eikonal time evolution equations (10) and (11), which were then solved numerically (Fig. 7). Here, the

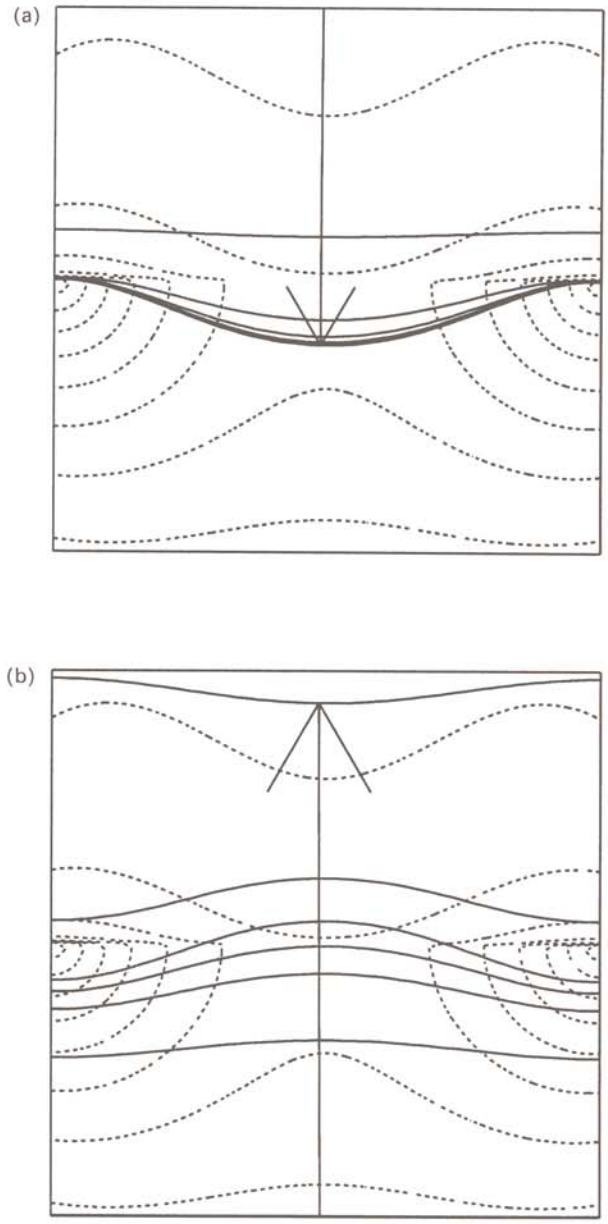

Figure 7. Spatially non-uniform tissue depression may induce a one-way block. Numerical solution of (10) and (11) with orthogonal boundary conditions on the domain $-1 \leqslant x, y \leqslant 1$, where $c^*(x^*, y^*)$ is given by (17) and $c_{\min} = -0.25$, shows how waves starting at the top of the domain ($y=1$, $-1 \leqslant x \leqslant 1$) are blocked (a), while waves starting at the bottom ($y=-1$, $-1 \leqslant x \leqslant 1$) sweep all the way up (b). Solid lines show the time evolution of the wave boundary, while dashed lines show constant c^* isoclines. The isoclines range from -0.20 (on the far left and right of centre) to $+0.15$ (at the top and bottom) by increments of 0.05.

solid lines show the time evolution of the wave boundary. We see that waves starting at the top of the domain ($y=1$, $-1\leqslant x\leqslant 1$) are blocked (Fig. 7a), while waves starting at the bottom ($y=-1$, $-1\leqslant x\leqslant 1$) sweep all the way up (Fig. 7b). Thus, spatially non-uniform depression of tissue may, in itself, be sufficient to induce a one-way block.

4. Discussion. Cranefield (1975) suggested that asymmetric conduction in cardiac fibres arises from spatial inhomogeneities in active and passive electrical properties of the fibres, from variations in the frequency and distribution of junctions and from directional asymmetries in the electrical pathway configurations in fibre networks. In terms of our eikonal equation model, the spatial variations in electrical properties and nexus junction locations suggest spatial dependence for the planar wave speed, c, while asymmetries in electrical pathway configurations may be commensurate with asymmetric domain geometry. Indicating that domain geometry (Section 2) and spatial dependence for c (Section 3) are key factors in causing asymmetric and one-way conduction, our results thus provide a theoretical framework which is in keeping with biological observations.

There are a number of auxiliary factors which may affect the depolarization wave speed in Purkinje fibres that have not been included in our model. These include time dependencies in the current–voltage relationship, the fact that the Purkinje fibre ultrastructure is species specific, the possibilities that the zero-flux boundary conditions on the system (3) may not be exact and that the fibre bundle is, in fact, comprised of discrete fibres which are electrotonically coupled in a manner which may be capacitive as well as resistive (Freygang and Trautwein, 1970). The fact that the current–voltage relationship may be changed substantially in Purkinje fibres which are depressed in a high K solution (Cranefield, 1975) does not affect the basic theory so long as fibres remain excitable, as no specific form was assumed for $f^*(V^*)$ in (5).

We have used the eikonal equation approximation (8) both as a conceptual and as a quantitative tool with which to model one-way blocks. Other quantitative models and simulations have used Huyghens' principle (see, for example, Auger *et al.*, 1988). In this case, $N=c$ and so no boundary conditions can be imposed. Here, the simulation of a one-way block requires the *a priori* imposition of one-way transmission in a given region. In our analysis we have shown that, in fact, it is the $\varepsilon\kappa$ correction to Huyghens' principle, given by the eikonal equation approximation, which is instrumental in causing the one-way block, thus rendering the artificial imposition of one-way transmission unnecessary.

We are grateful to Professor J. D. Murray for his encouragement and helpful comments.

LITERATURE

Allessie, M. A., F. I. M. Bonke and F. J. G. Schopman. 1977. Circus movement in rabbit atrial muscle as a mechanism of tachycardia. III. The 'leading circle' concept: a new model of circus movement in cardiac tissue without the involvement of an anatomical obstacle. *Circ. Res.* **41**, 9–18.

Ashman, R. and E. Hull. 1945. *Essentials of Electrocardiography*. New York: Macmillan.

Auger, P. M., A. Bardou, A. Coulombe and J. Degonde. 1988. Computer simulation of ventricular fibrillation. *Math. Comput. Model.* **11**, 813–822.

Beeler, G. W. and H. Reuter. 1977. Reconstruction of the action potential of ventricular myocardial fibers. *J. Physiol.* **268**, 177–210.

Chen, P. S., P. D. Wolf, E. G. Dixon, N. D. Daniely, D. W. Frazier, W. M. Smith and R. E. Ideker. 1988. Mechanism of ventricular vulnerability to single premature stimuli in open-chest dogs. *Circ. Res.* **62**, 1191–1209.

Clerc, L. 1976. Directional differences of impulse spread in trabecular muscle from mammalian heart. *J. Physiol.* **255**, 335–346.

Cranefield, P. F. 1975. *The Conduction of the Cardiac Impulse: The Slow Response and Cardiac Arrhythmias*, Chaps 2 and 5. New York: Futura.

Cranefield, P. F., H. O. Klein and B. F. Hoffman. 1971. Conduction of the cardiac impulse. I. Delay, block, and one-way block in depressed Purkinje fibers. *Circ. Res.* **28**, 199–219.

Freygang, W. H. and W. Trautwein. 1970. The structural implications of the linear electrical properties of cardiac Purkinje strands. *J. gen. Physiol.* **55**, 524–547.

Gomatam, J. and P. Grindrod. 1987. Three-dimensional waves in excitable reaction–diffusion systems. *J. math. Biol.* **25**, 611–622.

Grindrod, P., M. A. Lewis and J. D. Murray. 1991. A geometrical approach to wave-type solutions of excitable reaction–diffusion systems. *Proc. R. Soc. A* (in press).

Hunter, P. J., P. A. McNaughton and D. Noble. 1975. Analytical models of propagation in excitable cells. *Prog. biophys. Molec. Biol.* **30**, 99–144.

Jack, J. J. B., D. Noble and R. W. Tsien. 1975. *Electric Current Flow in Excitable Cells*. Oxford: Clarendon Press.

Johnson, E. A. and J. R. Sommer. 1967. A strand of cardiac muscle: its ultrastructure and the electrophysiological implications of its geometry. *J. Cell Biol.* **33**, 103–129.

Joyner, R. W. 1981. Mechanisms of unidirectional blocks in cardiac tissues. *Biophys. J.* **35**, 113–125.

Keener, J. P. 1984. Dynamic patterns in excitable media. In *Modelling of Patterns in Space and Time*, W. Jager and J. D. Murray (eds). Heidelberg: Springer-Verlag.

Keener, J. P. 1986. A geometrical theory for spiral waves in excitable media. *SIAM J. appl. Math.* **46**, 1039–1056.

Keener, J. P. 1987. Causes of propagation failure in excitable media. In *Temporal Disorder in Human Oscillatory Systems*, L. Rensing, U. an der Heiden and M. C. Mackey (eds), pp. 134–140. Berlin: Springer-Verlag.

McAllister, R. E., D. Noble and R. W. Tsien. 1975. Reconstruction of the electrical activity of cardiac Purkinje fibres. *J. Physiol.* **251**, 1–59.

Miller, R. N. 1979. A simple model of delay, block and one-way conduction in Purkinje fibers. *J. math. Biol.* **7**, 385–398.

Mobley, B. A. and E. Page. 1972. The surface area of sheep cardiac Purkinje fibers. *J. Physiol.* **220**, 547–563.

Noble, D. 1962. A modification of the Hodgkin–Huxley equations applicable to Purkinje fibre action and pace-maker potentials. *J. Physiol.* **160**, 317–352.

Schmitt, F. O. and J. Erlanger. 1928. Directional differences in the conduction of the impulse through heart muscle and their possible relation to extrasystolic and fibrillary contractions. *Am. J. Physiol.* **87**, 326–347.

Sommer, J. R. and E. A. Johnson. 1968. Cardiac muscle: a comparative study of Purkinje fibers and ventricular fibers. *J. Cell Biol.* **36**, 497–526.

Tyson, J. J. and J. P. Keener. 1987. Spiral waves in a model for the myocardium. *Physica* **D29**, 215–222.

Weidmann, S. 1952. The electrical constants of Purkinje fibres. *J. Physiol.* **118**, 348–360.

Winfree, A. T. 1983. Sudden cardiac death: a problem in topology. *Scient. Am.* **248** (5), 144–161.

Wit, A. L., B. F. Hoffman and P. F. Cranefield. 1972a. Slow conduction and re-entry in the ventricular conducting system. I. Return extrasystole in canine Purkinje fibers. *Circ. Res.* **30**, 1–10.

Wit, A. L., P. F. Cranefield and B. F. Hoffman. 1972b. Slow conduction and re-entry in the ventricular conducting system. II. Single and sustained circus movement in networks of canine and bovine Purkinje fibers. *Circ. Res.* **30**, 11–22.

Received 9 September 1990
Revised 30 November 1990